Direct Kerr electro-optic effect in noncentrosymmetric materials

Mike Melnichuk[1,*] and Lowell T. Wood[2]
[1]*Physics Department, University of Michigan, Ann Arbor, Michigan 48109-1040, USA*
[2]*Physics Department, University of Houston, Houston, Texas 77204-5005, USA*
(Received 6 November 2009; published 21 July 2010)

In materials lacking inversion symmetry, both Pockels and Kerr electro-optic effects are simultaneously present, with the former effect generally dominating the latter one. The theoretical findings of this article provide the crystal physics community with concrete tabulated evidence showing that it is possible in principle to selectively bypass contributions from the linear effect(s) and directly obtain information only about the genuine (Kerr-like) quadratic effects in 90% of the noncentrosymmetric point groups. The general idea and treatment used for the electro-optic effect can be extended and adapted to other optical or non-optical (phenomenological) purely quadratic effects in media lacking inversion symmetry.

DOI: 10.1103/PhysRevA.82.013821 PACS number(s): 42.70.Mp, 42.65.An, 42.25.Lc, 33.57.+c

I. INTRODUCTION

The electro-optic effect [1–35] becomes manifest when an electric field applied across a (dielectric) material induces changes in the optical refractive index(es) of the respective medium. In the most general case of an anisotropic biaxial crystal, the magnitude of the optical index of refraction varies with the direction in a material in such a way that its values generate an ellipsoid of rotation called the index ellipsoid or indicatrix, expressed, using Einstein's summation convention, as $n_{pq}^{-2}x_p x_q = 1$, $p,q = 1,2,3$, and $n_{pq}^{-2} = 0$ for $p \neq q$. With the application of an external vector field, the initial indicatrix degenerates into a new index ellipsoid expressed in the same initial system of principal axes as the quadratic form $n_{pq}'^{-2}x_p x_q = 1$. The relation between the index terms n'_{pq} and n_{pq} constitutes the electro-optic effect:

$$n_{pq}'^{-2} = n_{pq}^{-2} + r_{pqb}E_b + R_{pqbd}E_b E_d + \cdots, \tag{1}$$

where $\vec{E} = E_1\hat{x}_1 + E_2\hat{x}_2 + E_3\hat{x}_3$ is the electric field and $r_{pqb}E_b$, $R_{pqbd}E_b E_d$ are the Pockels and Kerr (electro-optic) terms, respectively.

The methods of detection in standard electro-optics involve the application of a low- or zero-frequency (DC) modulating electric field while the crystal is probed with a low-intensity polarized beam of light [2–21]. The usual electro-optical detection techniques are interferometric (Mach-Zehnder, Jamin, Michelson, and Fabry-Perot interferometers) [11–13,36], polarimetric (amplitude or phase modulators) [2–9,11–21], ellipsometric, and reflectometric [11]. In all these experimental situations, the intersection between the transversal polarization plane of the incident electromagnetic wave with the index ellipsoid generates a two-dimensional index ellipse $n_{pp}^{-2}x_p^2 + n_{qq}^{-2}x_q^2 = 1$ [Fig. 1(a)]. With the application of an electric field, the new index ellipse $n_{pp}'^{-2}x_p^2 + n_{qq}'^{-2}x_q^2 + 2n_{pq}'^{-2}x_p x_q = 1$ is reshaped and rotated [Fig. 1(b)]; the index terms n'_{pp},n'_{qq},n'_{pq} are connected to the initial refraction indexes n_{pp},n_{qq} and the Pockels and Kerr terms through the electro-optic effect [Eq. (1)]. In the new proper system of orthogonal coordinates $\hat{x}_{pq-}$,$\hat{x}_{pq+}$, the preceding quadratic form is reduced (diagonalized) to $n_{pq+}^{-2}x_{pq+}^2 + n_{pq-}^{-2}x_{pq-}^2 = 1$ [Fig. 1(c)], with the new (eigen)indexes of refraction n_{pq-} and n_{pq+} related to n'_{pp},n'_{qq},n'_{pq} by [21]

$$n_{pq\pm} = \left[\frac{1}{2}\left(n_{pp}'^{-2} + n_{qq}'^{-2}\right) \pm \frac{1}{2}\sqrt{\left(n_{pp}'^{-2} - n_{qq}'^{-2}\right)^2 + \left(2n_{pq}'^{-2}\right)^2}\right]^{-\frac{1}{2}}. \tag{2}$$

The effect also usually produces a rotation of the new index ellipse through an inclination angle θ_{pq} [Fig. 1(d)] connected to n'_{pp},n'_{qq},n'_{pq} by another exact formula [21]:

$$\tan(2\theta_{pq}) = \frac{2n_{pq}'^{-2}}{n_{pp}'^{-2} - n_{qq}'^{-2}}; \tag{3}$$

here $\theta_{pq} = -\theta_{qp}$ and $|\theta_{pq}| \leqslant 45^\circ$. In many cases, however, the inclination angle happens to remain null even after the application of the electric field. These special configurations could in principle be relatively straightforward to detect because, as will be shown in Sec. IV, in many of these relatively quite simple situations, a probing electromagnetic wave, initially polarized along one of the (eigen)axes, will maintain the direction of its initial state of polarization even after a voltage has been applied along a certain principal direction across the crystal.

In conventional electro-optics—which will be considered throughout this article—obtaining information about single or combinations of electro-optic terms is done through the determination of changes in the new optical phase(s) accumulated by the probing beam(s) of light when passing through or reflecting off a crystal; these (eigen)phases are directly proportional to the (eigen)indexes of refraction, which in turn are related through Eqs. (1)–(3) to the electro-optic effect. The present article will show that through a selective and simultaneous combination of three factors—crystal symmetry type, orientation and magnitude of the applied electric field, and propagation direction of the probing polarized light—it is possible in principle to detect only pure Kerr contributions in many noncentrosymmetric point groups generally exhibiting a simultaneous presence of both Pockels and Kerr effects with the linear (first-order) effect usually being the predominant one.

II. PRACTICAL APPROXIMATIONS

In practical applications, the (eigen)indexes of refraction are hardly ever used in their exact form(s) [Eq. (2)]; their

*mmeln@umich.edu

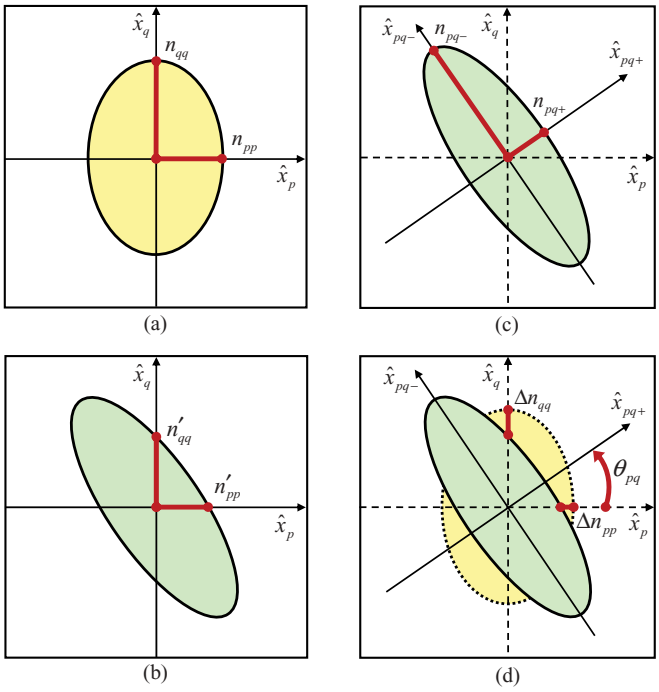

FIG. 1. (Color online) The two-dimensional geometry of the electro-optic effect. The probing light propagates normal (in)to the plane of the (article's) page. (a) The initial index ellipse of the unperturbed crystal; its intersection with the two Cartesian axes $\hat{x}_p,\hat{x}_q$ generates the two initial (eigen)indexes of refraction n_{pp},n_{qq}. (b) The new index ellipse induced by the application of an external electric field; its intersection points n'_{pp},n'_{qq} with the principal Cartesian axes $\hat{x}_p,\hat{x}_q$ are related to n_{pp},n_{qq} through the electro-optic effect [Eq. (1)]. (c) The new index ellipse in its proper system of orthogonal coordinates $\hat{x}_{pq+},\hat{x}_{pq-}$; its intersections generate the new (eigen)indexes of refraction n_{pq+},n_{pq-}. (d) The three (in-plane) geometrical changes that quantitatively characterize the existence of an electro-optic effect: $\Delta n_{pp}=n'_{pp}-n_{pp}$, $\Delta n_{qq}=n'_{qq}-n_{qq}$, and θ_{pq}. If at least one of these three parameters is nonzero, then the particular configuration indicates a potentially detectable electro-optic effect.

approximate expressions are mostly used instead because these usually happen to reveal important information concerning the net (overall) orders of magnitude of certain contributing electro-optic terms. In this section is provided a general approximation analysis of the (eigen)indexes of refraction for all three optical categories of noncentrosymmetric crystals, biaxial, uniaxial, and anaxial. In all anaxial and one-third of the uniaxial crystal configurations, the natural birefringence is zero ($n_{pp}=n_{qq}=n_o$); in the rest, two-thirds of the uniaxial and all biaxial cases, the natural birefringence is nonzero ($n_{pp},n_{qq}=n_e,n_o; n_{pp}\neq n_{qq}$ for $p\neq q$ simultaneously). Here n_o and n_e represent the ordinary and extraordinary indexes of refraction, respectively, of the unperturbed crystal.

All approximations that follow are based on two approximations related to the expression in Eq. (2). The first and commonly used one in electro-optics [2–21], $n_f^{-2}=n_i^{-2}+[\partial(n^{-2})/\partial n]|_i(n_f-n_i)+\cdots$, is a Taylor expansion of the (eigen)index(es) of refraction. By truncating it up to the first order and rearranging it, one gets the following: $n_f-n_i\cong-(n_i^3/2)(n_f^{-2}-n_i^{-2})\propto rE+RE^2$. The approximation is justified by the fact that the differences between the final (new) (eigen)index(es) of refraction (n_f) and the initial (old) principal refraction index(es) (n_i) are of the order of the electro-optic terms rE or RE^2. The r and R coefficients usually vary between 10^{-12} mV^{-1} and 10^{-9} mV^{-1} for Pockels and between 10^{-24} m^2 V^{-2} and 10^{-15} m^2 V^{-2} for Kerr (in mostly centrosymmetric materials) [2–9,11–13,22]. For an arbitrary electric field of the order 10^6 Vm^{-1}, the electro-optic contributions to the final (eigen)indexes of refraction will take values from around 10^{-6} to 10^{-3} for the Pockels terms and 10^{-12} to 10^{-3} for the Kerr terms, respectively, with the first-order (linear) terms always being relatively (much) greater than the second-order (quadratic) terms for the same type of noncentrosymmetric crystal. The second approximation, $\sqrt{1+\varepsilon}\cong 1+\varepsilon/2$ for $0\leqslant\varepsilon<1$, involves the truncated (binomial) expansion up to the first order of the square root in Eq. (2) $\sqrt{(n'^{-2}_{pp}-n'^{-2}_{qq})^2+(2n'^{-2}_{pq})^2}$; depending on which of the two terms inside the square root is relatively larger, $(n'^{-2}_{pp}-n'^{-2}_{qq})^2=[(n^{-2}_{pp}-n^{-2}_{qq})+(r_{ppb}-r_{qqb})E_b+(R_{ppbd}-R_{qqbd})E_bE_d]^2$ or $(2n'^{-2}_{pq})^2=4(r_{pqb}E_b+R_{pqbd}E_bE_d)^2$, the ε is either $[(2n'^{-2}_{pq})^2]/[(n'^{-2}_{pp}-n'^{-2}_{qq})^2]=\tan^2(2\theta_{pq})$ or $[(n'^{-2}_{pp}-n'^{-2}_{qq})^2]/[(2n'^{-2}_{pq})^2]=\tan^{-2}(2\theta_{pq})$, respectively. Aside from the extreme cases when ε is either 0 or 1, and based on what can be inferred from the electro-optics literature [2–9,11–13,22], ε usually varies in magnitude from 10^{-24} to 10^{-2}.

In the zero-natural-birefringence situations, for $|2n'^{-2}_{pq}|\leqslant|n'^{-2}_{pp}-n'^{-2}_{qq}|$ or $|\theta_{pq}|\leqslant 22.5^\circ$, Eq. (2) can be approximated by

$$n_{pq+/-}\cong n_o-\frac{n_o^3}{2}\left(n'^{-2}_{pp/qq}-n_o^{-2}+/-\frac{n'^{-4}_{pq}}{n'^{-2}_{pp}-n'^{-2}_{qq}}\right), \quad (4)$$

and for $|n'^{-2}_{pp}-n'^{-2}_{qq}|<|2n'^{-2}_{pq}|$ or $22.5^\circ<|\theta_{pq}|\leqslant 45^\circ$, by

$$n_{pq\pm}\cong n_o-\frac{n_o^3}{4}\left[n'^{-2}_{pp}+n'^{-2}_{qq}-2n_o^{-2}\pm 2n'^{-2}_{pq}\pm\frac{\left(n'^{-2}_{pp}-n'^{-2}_{qq}\right)^2}{4n'^{-2}_{pq}}\right]. \quad (5)$$

In the two preceding expressions, we take $(n'^{-2}_{pp}-n'^{-2}_{qq})^2=[(R_{ppbd}-R_{qqbd})E_bE_d]^2$ and $n'^{-4}_{pq}=(R_{pqbd}E_bE_d)^2$, with $n_{pp}=n_{qq}=n_o$ ($p\neq q$); as a rule, only cases containing overall Kerr-like (genuine) quadratic dependencies (10^{-12}–10^{-3}) will be considered in this article. If, however, in a hypothetical scenario, either one of index terms $n'^{-2}_{pp},n'^{-2}_{qq},n'^{-2}_{pq}$ happens to contain at least one Pockels term, then Eqs. (4) and (5) show that this term will reveal itself conspicuously in the new (eigen)indexe(s) of refraction. Therefore the only consistent way of having just net quadratic contributions in the zero-natural-birefringence situations is that the preceding index terms all be simultaneously free of any Pockels terms.

In the nonzero-natural-birefringence cases ($n_{pp},n_{qq}=n_o,n_e$, $n_{pp}\neq n_{qq}$, $p\neq q$), the difference term $n_{pp}^{-2}-n_{qq}^{-2}\cong n'^{-2}_{pp}-n'^{-2}_{qq}=n_{pp}^{-2}-n_{qq}^{-2}+(R_{ppbd}-R_{qqbd})E_bE_d$ is, for all practical purposes, much greater than any electro-optic effect contributions ($>10^{-3}\gg 10^{-12}$); this leads to the only realistic situation(s) for these types of cases: $|2n'^{-2}_{pq}|\leqslant|n'^{-2}_{pp}-n'^{-2}_{qq}|$ or

$|\theta_{pq}| < 22.5^{\circ}$. The (eigen)indexes of refraction given in Eq. (2) are now approximated by

$$n_{pq+/-} \cong n_{pp/qq} - \frac{n_{pp/qq}^{3}}{2}\left(n_{pp/qq}^{\prime -2} - n_{pp/qq}^{-2} + / - \frac{n_{pq}^{\prime -4}}{n_{pp}^{\prime -2} - n_{qq}^{\prime -2}}\right). \tag{6}$$

As in the previous paragraph, if any of the homogeneous index terms $n_{pp}^{\prime -2}, n_{qq}^{\prime -2}$ contains at least one Pockels coefficient, then the corresponding linear (electro-optic) term(s) associated with them will automatically be revealed prominently in the (eigen)indexes of refraction [Eq. (6)]. The same is no longer valid here for the inhomogeneous index term $n_{pq}^{\prime -2}$; by considering a Pockels effect in $n_{pq}^{\prime -2}$ ($n_{pq}^{\prime -2} = r_{pqb}E_b + R_{pqbd}E_bE_d$), Eq. (6) becomes

$$n_{pq+/-} \cong n_{pp/qq} - \frac{n_{pp/qq}^{3}}{2}\left[n_{pp/qq}^{\prime -2} - n_{pp/qq}^{-2} + / - \frac{(r_{pqb}E_b + R_{pqbd}E_bE_d)^2}{n_{pp}^{\prime -2} - n_{qq}^{\prime -2}}\right]. \tag{7}$$

When dealing with quadratic electro-optic effects in nonzero-natural-birefringence situations, the mixed (subscript) term(s) of the form $n_{pq}^{\prime -4}$ can introduce refractive index(es) dependencies which are quartic, $(R_{pqbd}E_bE_d)^2$, cubic, $2(r_{pqb}E_b)(R_{pqbd}E_bE_d)$, and quadratic, $(r_{pqb}E_b)^2$, in the electric field(s). From all these contributions, only the latter is important enough not to be neglected in certain (quadratic) configurations [37]; although worthy of explicit particular attention [38] mainly because of its comparable order of magnitude (10^{-12}–10^{-6}) relative to the Kerr effect, this inconspicuous quadratic contribution is merely due to the squaring of certain Pockels term(s) and, for that matter, is not of an authentic Kerr-like quadratic nature.

In the present theoretical work, the authors provide the extensive and concrete treatment of only the genuine quadratic (electro-optic) effect, involving just (combinations of) Kerr coefficients (moduli) alone, in media lacking inversion symmetry; the most reliable way of achieving this is by methodically selecting only the electro-optic configurations which allow for the three index terms $n_{pp}^{\prime -2}, n_{qq}^{\prime -2}, n_{pq}^{\prime -2}$ ($p \neq q$) to be simultaneously devoid of any Pockels terms while making sure that Eqs. (2) and (3) will contain at least one (nonzero) Kerr contribution.

III. CONCRETE EXAMPLE

The previous claim is clarified through a concrete example which provides explicitly the exact and corresponding approximate expressions for a pair of (eigen)indexes of refraction and inclination angles containing only (combinations of) Kerr terms in a noncentrosymmetric (uniaxial) crystal.

We consider the particular configuration of a tetragonal $4mm$ point group symmetry crystal, such as the ferroelectric barium titanate ($BaTiO_3$), with an externally applied electric field of the form $\vec{E} = E_1\hat{x}_1 + E_2\hat{x}_2$. The direction of the probing light beam $\hat{k}$ coincides with $\hat{x}_3$; this makes the transversal polarization plane of the electromagnetic wave parallel to the $\hat{x}_1\hat{x}_2$ plane of the index ellipse. In this case, the electro-optic effect for the tetragonal $4mm$ class can be captured in its most explicitly revealing format by a matrix equation of the form

$$\begin{bmatrix} n_1^{\prime -2} \\ n_2^{\prime -2} \\ n_3^{\prime -2} \\ n_4^{\prime -2} \\ n_5^{\prime -2} \\ n_6^{\prime -2} \end{bmatrix} = \begin{bmatrix} n_o^{-2} \\ n_o^{-2} \\ n_e^{-2} \\ 0 \\ 0 \\ 0 \end{bmatrix} + \begin{bmatrix} 0 & 0 & r_{13} \\ 0 & 0 & r_{13} \\ 0 & 0 & r_{33} \\ 0 & r_{51} & 0 \\ r_{51} & 0 & 0 \\ 0 & 0 & 0 \end{bmatrix} \begin{bmatrix} E_1 \\ E_2 \\ 0 \end{bmatrix} + \begin{bmatrix} R_{11} & R_{12} & R_{13} & 0 & 0 & 0 \\ R_{12} & R_{11} & R_{13} & 0 & 0 & 0 \\ R_{31} & R_{31} & R_{33} & 0 & 0 & 0 \\ 0 & 0 & 0 & R_{44} & 0 & 0 \\ 0 & 0 & 0 & 0 & R_{44} & 0 \\ 0 & 0 & 0 & 0 & 0 & R_{66} \end{bmatrix} \begin{bmatrix} E_1^2 \\ E_2^2 \\ 0 \\ 0 \\ 0 \\ E_1E_2 \end{bmatrix}. \tag{8}$$

The ordinary (n_o) and extraordinary (n_e) refractive indexes are always assumed to be known in this article. For the sake of simplicity, the standard tensor subscript compression convention was used: $11 \rightarrow 1$, $22 \rightarrow 2$, $33 \rightarrow 3$, $23 = 32 \rightarrow 4$, $13 = 31 \rightarrow 5$, $12 = 21 \rightarrow 6$. The 3×6 matrix contains the Pockels coefficients, while the 6×6 matrix contains the Kerr moduli [2,7,8]. For the particular configuration chosen ($p = 1$, $q = 2$), the only relevant equations are the ones involving the subscripts $11 \rightarrow 1$, $22 \rightarrow 2$, and $12 = 21 \rightarrow 6$; these make the top two rows and the bottom row in Eq. (8). The new (eigen)indexes of refraction and inclination angle are then obtained using Eqs. (2) and (3):

$$n_{12\pm} = \left[n_o^{-2} + \frac{1}{2}(R_{11} + R_{12})\left(E_1^2 + E_2^2\right) \pm \frac{1}{2}\sqrt{(R_{11} - R_{12})^2\left(E_1^2 - E_2^2\right)^2 + 4R_{66}^2E_1^2E_2^2}\right]^{-\frac{1}{2}}, \tag{9}$$

$$\tan(2\theta_{12}) = \frac{2R_{66}E_1E_2}{(R_{11} - R_{12})\left(E_1^2 - E_2^2\right)}. \tag{10}$$

When either E_1 or E_2 is zero without both being null simultaneously, $|\theta_{12}|$ reaches its minimum value of 0°; for $E_1 = \pm E_2 \neq 0\,\mathrm{V m^{-1}}$, $|\theta_{12}|$ reaches its maximum value of 45°. To be noticed is the fact that the two exact expressions above [Eqs. (9) and (10)] contain absolutely no Pockels coefficients in them; all contributions due to the generally preponderant first-order (linear) electro-optic effect for the uniaxial tetragonal $4mm$ point group class have been completely bypassed in this particular optical configuration.

The example provided here falls into the zero-natural-birefringence category for uniaxial crystal configurations discussed in the previous section [Eqs. (4) and (5)]. The

(eigen)indexes of refraction in Eq. (9) can be approximated by

$$n_{12+/-} \cong n_o - \frac{n_o^3}{2}\left[R_{11/12}E_1^2 + R_{12/11}E_2^2 \right. \\ \left. +/- \frac{R_{66}^2 E_1^2 E_2^2}{(R_{11}-R_{12})\left(E_1^2 - E_2^2\right)}\right], \qquad (11)$$

when $|2R_{66}E_1E_2| \leqslant |(R_{11}-R_{12})(E_1^2-E_2^2)|$ or $|\theta_{12}| \leqslant 22.5^\circ$ and by

$$n_{12\pm} \cong n_o - \frac{n_o^3}{4}\left[(R_{11}+R_{12})\left(E_1^2+E_2^2\right) \pm 2R_{66}E_1E_2 \right. \\ \left. \pm \frac{(R_{11}-R_{12})^2\left(E_1^2-E_2^2\right)^2}{4R_{66}E_1E_2}\right], \qquad (12)$$

for $|(R_{11}-R_{12})(E_1^2-E_2^2)| < |2R_{66}E_1E_2|$ or $22.5^\circ < |\theta_{12}| \leqslant 45^\circ$.

The last (fractional) terms in the preceding approximations [Eqs. (11) and (12)] have an overall quadratic influence on the new indexes of refraction, although their numerators reveal a quartic dependence on the applied electric field because of the squaring of the Kerr term(s). In all the zero-natural-birefringence approximations mentioned in the previous section [Eqs. (4) and (5)], these (last) fractional types of terms introduce net quadratic contributions (10^{-12}–10^{-3}) which cannot be neglected in situations dealing with an authentic second-order electro-optic effect.

IV. EXPERIMENTAL SCHEMATIC

The sketch of a new electro-optic experimental setup (Fig. 2) is presented here and then theoretically applied to an even simpler tetragonal 4*mm* configuration with the purpose of showing how certain (pure) Kerr coefficients can in principle be directly determined in noncentrosymmetric crystals. For the sake of clarity of purpose, the treatment of the electromechanical coupling effect of electrostriction associated with the quadratic electro-optic effect will be kept to a minimum of detail. In its bare-essentials format, the design proposed here combines a Mach-Zehnder interferometer (top left corner), a Michelson interferometer (bottom right corner), and an amplitude-modulated null polarimeter (top right corner) in a three-in-one compact arrangement.

The light generated by a low-power laser (L) of wavelength λ is (linearly) polarized by a (high-extinction-ratio) polarizer P before being split by one of the four (antireflection-coated and nonpolarizing) beamsplitters (BS1); the source's light intensity is in permanence monitored at the bottom left corner of the experimental setup by one of the three (high-sensitivity) power detectors (D3). The Mach-Zehnder interferometer and the (null) polarimeter can be used in parallel to measure the change in the electrically induced birefringence of the (crystal) sample (S) in transmission; in this particular setup (Fig. 2), however, the polarimeter is used only for proper alignment of the crystal across the incident ray of light. One of the two (pairs of) beams exiting beamsplitter BS3 generates an interference pattern which is captured with one of the two (high-resolution)

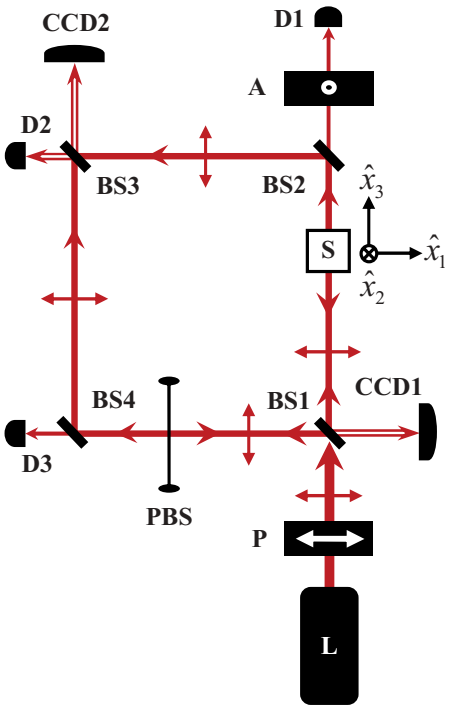

FIG. 2. (Color online) Experimental schematic of the direct Kerr electro-optic effect in noncentrosymmetric crystals. The experimental setup combines a Mach-Zehnder interferometer (top left corner), a Michelson interferometer (bottom right corner), and an amplitude-modulated null polarimeter (top right corner) in a three-in-one compact design. BS1, BS2, BS3, and BS4 are similar antireflection-coated and nonpolarizing beamsplitters; D1, D2, D3 and CCD1, CCD2 are similar high-sensitivity power detectors and similar high-resolution CCD-CMOS cameras, respectively. L, S, and PBS are a low-power laser, the (crystal) sample, and a no-multiple-reflections and nonpolarizing pellicle beamsplitter, respectively. P and A are two similar high-extiction rate polarizers oriented at 90° to each other in a null format.

CCD-CMOS cameras (CCD2) and later analyzed; the other beam is used to real-time monitor the (light) intensity in the Mach-Zehnder interferometer with the use of detector D2. The same type of power detector (D1) is used to monitor the amount of light that passes through the (high-extinction-ratio) null analyzer (A) when the electric field is on. The Michelson interferometer is used for simultaneous measurement of the change in the sample's thickness with the application of a voltage across it—the electromechanical effect; the fringe pattern generated by the interference between the part of the (right) incident beam reflecting off the sample's surface and the part of the (left) incident beam reflecting off the (no-multiple-reflections and nonpolarizing) pellicle beamsplitter (PBS) are captured with CCD1 and analyzed. Here the shift in the reflection fringes (δ_R) is directly proportional to the phase change $\Delta\varphi_R = (2\pi/\lambda)\Delta\ell_3$ suffered by the two (reflected) interfering waves; this phase difference, in turn, is related to the change in the thickness of the sample ($\Delta\ell_3$) along the $\hat{x}_3$ direction. The fringe shift generated at the Michelson interferometer (CCD1) by the two beams (Fig. 2) is (directly) proportional to $\Delta\ell_3$:

$$\delta_R \propto \Delta\ell_3. \qquad (13)$$

We shall now consider the previous theoretical example (Sec. III) in the even simpler event when $E_2 = 0\ \mathrm{Vm}^{-1}$ and $E_1 \neq 0\ \mathrm{Vm}^{-1}$. For a polarized wave propagating along the $\hat{k} = \hat{x}_3$ axis and having its linear polarization parallel to the applied electric field in the $\hat{x}_1$ direction (Fig. 2), the (eigen)index of refraction that the light beam now sees is the correspondingly reduced version of Eq. (11):

$$n_{12+} = n_1' \cong n_o - \frac{n_o^3}{2} R_{11} E_1^2. \tag{14}$$

The inclination angle remains unchanged in this case ($\theta_{12} = 0^\circ$). The fringe shift in transmission (δ_T) measured by the CCD2 is directly proportional to the phase difference $\Delta\varphi_T \cong (2\pi/\lambda)[\Delta n_{12+}\ell_3 + (n_o - 1)\Delta\ell_3]$ [13]; this phase change in transmission through the material ($\Delta\varphi_T$) is in turn related to the electrically induced variation of the (eigen)index of refraction ($\Delta n_{12+} = \Delta n_1 = n_{12+} - n_o$) along $\hat{x}_1$, the change in the thickness of the sample ($\Delta\ell_3$), and the initial thickness (ℓ_3) of the virgin crystal. The fringe shift generated at the Mach-Zehnder interferometer (CCD2) by the two beams (Fig. 2) is (directly) proportional to

$$\delta_T \propto \Delta n_{12+}\ell_3 + (n_o - 1)\Delta\ell_3. \tag{15}$$

Combining Eqs. (13)–(15), we end up with an expression of (direct) proportionality between the Kerr coefficient $R_{11} = R_{22}$ for the uniaxial tetragonal $4mm$ point group and the (difference between) measurable fringe shifts in transmission (Mach-Zehnder interferometer) and reflection (Michelson interferometer), respectively, for a given applied electric field (E_1):

$$R_{11} \propto \frac{2}{n_o^3 \ell_3}\left[\frac{(n_o - 1)\delta_R - \delta_T}{E_1^2}\right]. \tag{16}$$

In the low-field-strength (phenomenological) treatment of the electro-optic effect, the (Kerr) coefficients are independent of the magnitude of the perturbing field(s); in other words, for (DC) fields of a few hundred volts per millimeter, the fractional term in the square brackets in Eq. (16) remains constant for the same type of crystal (n_o) having the same initial thickness (ℓ_3) and being probed in the same direction with the same type of light characteristics (λ). The same approach can be used to directly determine $R_{12} = R_{21}$ for the same symmetry class configuration either by applying the electric field in the $\hat{x}_2$ direction ($E_2 \neq 0\ \mathrm{Vm}^{-1}$, $E_1 = 0\ \mathrm{Vm}^{-1}$), which happens to point normal (in)to the plane of the (article's) page in Fig. 2, or simply by rotating the (null) polarizer-analyzer complex by 90° without changing the direction or the magnitude of the initially applied electric field. So in these two simple and in-plain-sight configurations [Eq. (8)], by measuring the two fringe shifts (δ_T, δ_R), it is possible to directly determine the individual values of the two (different) Kerr coefficients (R_{11}, R_{12}) for $4mm$ $BaTiO_3$ in a relatively straightforward manner.

In the situation mentioned earlier, it was assumed that the direction of light polarization is already oriented along one of the principal axes of the undisturbed crystal. In practice, good alignment of the index ellipsoid relative to the polarization direction of the beam can be achieved using the null polarimeter in the top right corner of Fig. 2 and a sample rotating-tilting stage having high angular resolution (<0.0003°) [39,40]. For a null amplitude modulator, the intensity (I) measured by D1 has the well-known form [2–4]

$$I = I_{\max} \sin^2\left(\frac{\pi \Delta n \ell_3}{\lambda}\right). \tag{17}$$

$I_{\max}$ is the maximum intensity through the polarimeter, and Δn is the apparent natural birefringence in the $\hat{x}_1\hat{x}_2$ plane of the misaligned virgin sample. When properly aligned, an uniaxial crystal (tetragonal $4mm$) having its optical axis (n_e) along $\hat{x}_3$ will show no natural birefringence in the $\hat{x}_1\hat{x}_2$ plane ($\Delta n = n_o - n_o = 0$), and the transmitted intensity in Eq. (17) becomes zero; this implies that in practice, the lowest intensity reading at the (null) amplitude modulator will usually correspond to a well-aligned initial sample. As an additional precautionary measure, preliminary testing for proper orientation of the indicatrix relative to the cut faces of the virgin crystal can be done using conoscopic imaging techniques commonly used in optical crystallography and mineralogy [41,42].

The two interferometers can also be used to detect any unwanted accidental appearance of a linear electro-optic and/or electromechanical effect during measurements. These first-order effects make themselves manifest by the way the interference fringes shift; in the case of a net linear effect, the fringe(s) will spatially oscillate (left and right) around the initial position(s) corresponding to the electrically unperturbed crystal every time the voltage polarity across the sample switches sign. This is not the case when a quadratic effect becomes the outstanding one; with no linear effect creeping in, the (final) positions of the fringes remain independent of the polarity of the applied electric field as long as its (maximum) amplitude remains constant in magnitude. So this fringe shift feature can be used in addition to the null polarimeter technique mentioned earlier to ensure that the crystal remains properly aligned and that no (residual) first-order effect compromises the detection of a (genuine) quadratic one. Furthermore, the collection of two-dimensional interference patterns on CCD-CMOS cameras at the two interferometers can always facilitate the early detection of any electrically induced precursor effects and irregularities such as twinning in the volume or at the surface of the sample. Any local sharp contrast variations (spikes or dips) in the (continuous) intensity profile of the interference patterns may indicate the possibility of something experimentally compromising happening to the sample under test; these together with changes in the intensity at D2 and D1, respectively, and without any variations in it at D3, can be good early-warning indicators of (irreversible) crystal damage. On a final note, having two other similar optical arrangements, as the (full) design in Fig. 2 only rotated at 90° relative to each other and the present one, and functioning in conjunction with it, while simultaneously probing the crystal in the extra $\hat{x}_1$ and $\hat{x}_2$ directions, constitutes one of the most complete ways of measuring the (electro-optic) properties of a crystal sample while monitoring its alignment and physical (quality) status before and during the application of a voltage across it.

V. RESULTS AND DISCUSSION

The 20 noncentrosymmetric crystal classes have been systematically analyzed and the results tabulated in Table I

for all the theoretical configurations allowing for ways of selectively exploiting the symmetries of the point groups in order to avoid any (camouflaged) involvements of Pockels moduli. Interestingly enough, it has been found that aside from the (biaxial) triclinic 1 and (uniaxial) trigonal 3, it is possible in principle to directly detect at least one pure Kerr contribution

TABLE I. Configurations for direct determination of Kerr electro-optic coefficients in noncentrosymmetric crystals. The unit vector $\hat{k}$ represents the direction of propagation for the probing beam of light; here it is always taken to be along one of the principal Cartesian axes $\hat{x}_1$, $\hat{x}_2$, or $\hat{x}_3$. The components of the externally applied electric field $\vec{E} = E_1\hat{x}_1 + E_2\hat{x}_2 + E_3\hat{x}_3$ which are not present in a particular table cell are considered to be zero by default. Variable θ_{pq} is the inclination angle of the index ellipse; it is located in the $\hat{x}_p\hat{x}_q$ plane, which coincides with the transversal polarization plane of the incident light wave for each particular configuration. The Rs represent the Kerr coefficients. The bar-on-top (Kerr) moduli ($\bar{R}$) belong to electro-optic terms which introduce overall quartic contributions (10^{-24}–10^{-6}) to the new (eigen)indexes of refraction in the nonzero-natural-birefringence approximations [Eqs. (6) and (7)]. The initial refractive indexes are considered to be known, with the extraordinary indexes of refraction n_e always along the $\hat{x}_3$ axis. The abbreviation HOC applies to higher-order (electro-optic) moduli beginning with third-order (cubic) ones.

$\hat{k}$	$\vec{E}$	θ_{pq}	Electro-optic coefficients
		Noncentrosymmetric-biaxial-monoclinic $m(m\perp\hat{x}_2)$	
$\hat{x}_2$	E_2	$0^\circ < \lvert\theta_{13}\rvert < 22.5^\circ$	$R_{12}, R_{32}, \bar{R}_{52}$
		Noncentrosymmetric-biaxial-monoclinic $m(m\perp\hat{x}_3)$	
$\hat{x}_3$	E_3	$\theta_{12} = 0^\circ$	R_{13}, R_{23}
		Noncentrosymmetric-biaxial-monoclinic $2(2 \parallel \hat{x}_2)$	
$\hat{x}_2$	E_1, E_3	$0^\circ < \lvert\theta_{13}\rvert < 22.5^\circ$	$R_{11}, R_{31}, R_{13}, R_{33}, R_{15}, R_{35}\bar{R}_{51}, \bar{R}_{53}, \bar{R}_{55}$
		Noncentrosymmetric-biaxial-monoclinic $2(2 \parallel \hat{x}_3)$	
$\hat{x}_3$	E_1, E_2	$0^\circ \leqslant \lvert\theta_{12}\rvert < 22.5^\circ$	$R_{11}, R_{21}, R_{12}, R_{22}, \bar{R}_{66}$
		Noncentrosymmetric-biaxial-orthorhombic $2mm$	
$\hat{x}_1$	E_1	$\theta_{23} = 0^\circ$	R_{21}, R_{31}
$\hat{x}_2$	E_2	$\theta_{13} = 0^\circ$	R_{12}, R_{32}
$\hat{x}_3$	E_1, E_2	$0^\circ \leqslant \lvert\theta_{12}\rvert < 22.5^\circ$	$R_{11}, R_{21}, R_{12}, R_{22}, \bar{R}_{66}$
		Noncentrosymmetric-biaxial-orthorhombic 222	
$\hat{x}_1$	E_2, E_3	$0^\circ \leqslant \lvert\theta_{23}\rvert < 22.5^\circ$	$R_{22}, R_{32}, R_{23}, R_{33}, \bar{R}_{44}$
$\hat{x}_2$	E_1, E_3	$0^\circ \leqslant \lvert\theta_{13}\rvert < 22.5^\circ$	$R_{11}, R_{31}, R_{13}, R_{33}, \bar{R}_{55}$
$\hat{x}_3$	E_1, E_2	$0^\circ \leqslant \lvert\theta_{12}\rvert < 22.5^\circ$	$R_{11}, R_{21}, R_{12}, R_{22}, \bar{R}_{66}$
		Noncentrosymmetric-uniaxial-trigonal $3m(m\perp\hat{x}_1)$	
$\hat{x}_1$	E_1	$0^\circ < \lvert\theta_{23}\rvert < 22.5^\circ$	$R_{21}, R_{31}, \bar{R}_{41}$; $R_{12}, R_{13}, R_{23}, R_{32}, \bar{R}_{42}, \bar{R}_{56}$
		Noncentrosymmetric-uniaxial-trigonal $3m(m\perp\hat{x}_2)$	
$\hat{x}_2$	E_2	$\theta_{13} = 0^\circ$	R_{12}, R_{32}; $R_{21}, R_{31}, R_{13}, R_{23}$
		Noncentrosymmetric-uniaxial-trigonal 32	
$\hat{x}_1$	E_2, E_3	$0^\circ \leqslant \lvert\theta_{23}\rvert < 22.5^\circ$	$R_{22}, R_{32}, R_{23}, R_{33}, R_{24}, \bar{R}_{42}, \bar{R}_{44}$; $R_{11}, R_{31}, R_{13}, R_{14}, \bar{R}_{41}, \bar{R}_{55}, \bar{R}_{56}, R_{65}$
$\hat{x}_2$	E_3	$\theta_{13} = 0^\circ$	R_{13}, R_{33}; R_{23}, R_{31}, R_{32}
$\hat{x}_3$	E_3	θ_{12} is indeterminate	R_{13}, HOC; R_{23}, R_{31}, R_{32}
		Noncentrosymmetric-uniaxial-tetragonal $4mm$	
$\hat{x}_1$	E_1	$\theta_{23} = 0^\circ$	R_{21}, R_{31}; R_{12}, R_{32}
$\hat{x}_2$	E_2	$\theta_{13} = 0^\circ$	R_{12}, R_{32}; R_{21}, R_{31}
$\hat{x}_3$	E_1, E_2	$0^\circ \leqslant \lvert\theta_{12}\rvert \leqslant 45^\circ$	R_{11}, R_{12}, R_{66}; R_{22}, R_{21}
		Noncentrosymmetric-uniaxial-tetragonal 4 and $\bar{4}$	
$\hat{x}_3$	E_1	$\theta_{12} = \frac{1}{2}\arctan(\frac{2R_{61}}{R_{11}-R_{21}})$	R_{11}, R_{21}, R_{61}; R_{22}, R_{12}, R_{62}
$\hat{x}_3$	E_2	$\theta_{12} = \frac{1}{2}\arctan(\frac{2R_{62}}{R_{12}-R_{22}})$	R_{12}, R_{22}, R_{62}; R_{21}, R_{11}, R_{61}
$\hat{x}_3$	$E_1 = \pm E_2$	$\theta_{12} = \frac{1}{2}\arctan(\frac{R_{66}}{R_{16}})$	$R_{11}, R_{12}, R_{16}, R_{66}$; R_{22}, R_{21}, R_{26}
$\hat{x}_3$	E_1, E_2	$0^\circ \leqslant \lvert\theta_{12}\rvert \leqslant 45^\circ$	$R_{11}, R_{12}, R_{16}, R_{61}, R_{66}$; $R_{22}, R_{21}, R_{26}, R_{62}$
		Noncentrosymmetric-uniaxial-tetragonal $\bar{4}2m(2 \parallel \hat{x}_1)$	
$\hat{x}_1$	E_2, E_3	$0^\circ \leqslant \lvert\theta_{23}\rvert < 22.5^\circ$	$R_{22}, R_{23}, R_{32}, R_{33}, \bar{R}_{44}$; $R_{11}, R_{13}, R_{31}, \bar{R}_{55}$
$\hat{x}_2$	E_1, E_3	$0^\circ \leqslant \lvert\theta_{13}\rvert < 22.5^\circ$	$R_{11}, R_{13}, R_{31}, R_{33}, \bar{R}_{55}$; $R_{22}, R_{23}, R_{32}, \bar{R}_{44}$
$\hat{x}_3$	E_1, E_2	$0^\circ \leqslant \lvert\theta_{12}\rvert \leqslant 45^\circ$	R_{11}, R_{12}, R_{66}; R_{21}, R_{22}

TABLE I. (*Continued*.)

$\hat{k}$	$\vec{E}$	θ_{pq}	Electro-optic coefficients
		Noncentrosymmetric-uniaxial-tetragonal 422	
$\hat{x}_1$	E_2, E_3	$0^\circ \leqslant \lvert\theta_{23}\rvert < 22.5^\circ$	$R_{22}, R_{23}, R_{32}, R_{33}, \bar{R}_{44}; R_{11}, R_{13}, R_{31}, \bar{R}_{55}$
$\hat{x}_2$	E_1, E_3	$0^\circ \leqslant \lvert\theta_{13}\rvert < 22.5^\circ$	$R_{11}, R_{13}, R_{31}, R_{33}, \bar{R}_{55}; R_{22}, R_{23}, R_{32}, \bar{R}_{44}$
$\hat{x}_3$	E_3	θ_{12} is indeterminate	R_{13}, HOC; R_{23}
$\hat{x}_3$	E_1, E_2	$0^\circ \leqslant \lvert\theta_{12}\rvert \leqslant 45^\circ$	$R_{11}, R_{12}, R_{66}; R_{21}, R_{22}$
$\hat{x}_3$	E_1, E_2, E_3	$0^\circ \leqslant \lvert\theta_{12}\rvert \leqslant 45^\circ$	$R_{11}, R_{12}, R_{13}, R_{66}; R_{21}, R_{22}, R_{23}$
		Noncentrosymmetric-uniaxial-hexagonal 6	
$\hat{x}_3$	E_1	$\theta_{12} = \frac{1}{2}\arctan(\frac{2R_{61}}{R_{11}-R_{21}})$	$R_{11}, R_{21}, R_{61}; R_{22}, R_{12}, R_{16}, R_{26}, R_{62}, R_{66}$
$\hat{x}_3$	E_2	$\theta_{12} = \frac{1}{2}\arctan(\frac{2R_{62}}{R_{12}-R_{22}})$	$R_{12}, R_{22}, R_{62}; R_{21}, R_{11}, R_{26}, R_{16}, R_{61}, R_{66}$
$\hat{x}_3$	$E_1 = \pm E_2$	$\theta_{12} = \frac{1}{2}\arctan(\frac{R_{12}-R_{11}}{2R_{61}})$	$R_{11}, R_{21}, R_{61}; R_{22}, R_{12}, R_{16}, R_{26}, R_{62}, R_{66}$
$\hat{x}_3$	E_1, E_2	$0^\circ \leqslant \lvert\theta_{12}\rvert \leqslant 45^\circ$	$R_{11}, R_{21}, R_{61}; R_{22}, R_{12}, R_{16}, R_{26}, R_{62}, R_{66}$
		Noncentrosymmetric-uniaxial-hexagonal $\bar{6}$	
$\hat{x}_1$	E_3	$\theta_{23} = 0^\circ$	$R_{23}, R_{33}; R_{13}$
$\hat{x}_2$	E_3	$\theta_{13} = 0^\circ$	$R_{13}, R_{33}; R_{23}$
$\hat{x}_3$	E_3	θ_{12} is indeterminate	R_{13}, HOC; R_{23}
		Noncentrosymmetric-uniaxial-hexagonal 622	
$\hat{x}_1$	E_2, E_3	$0^\circ \leqslant \lvert\theta_{23}\rvert < 22.5^\circ$	$R_{22}, R_{23}, R_{32}, R_{33}, \bar{R}_{44}; R_{11}, R_{13}, R_{31}, \bar{R}_{55}$
$\hat{x}_2$	E_1, E_3	$0^\circ \leqslant \lvert\theta_{13}\rvert < 22.5^\circ$	$R_{11}, R_{13}, R_{31}, R_{33}, \bar{R}_{55}; R_{22}, R_{23}, R_{32}, \bar{R}_{44}$
$\hat{x}_3$	E_3	θ_{12} is indeterminate	R_{13}, HOC; R_{23}
$\hat{x}_3$	E_1, E_2	$\theta_{12} = \frac{1}{2}\arctan(\frac{E_1E_2}{E_1^2-E_2^2})$	$R_{11}, R_{12}; R_{21}, R_{22}, R_{66}$
$\hat{x}_3$	E_1, E_2, E_3	$\theta_{12} = \frac{1}{2}\arctan(\frac{E_1E_2}{E_1^2-E_2^2})$	$R_{11}, R_{12}, R_{13}; R_{21}, R_{22}, R_{23}, R_{66}$
		Noncentrosymmetric-uniaxial-hexagonal $\bar{6}m2(m\perp\hat{x}_1)$	
$\hat{x}_1$	E_1, E_3	$\theta_{23} = 0^\circ$	$R_{21}, R_{31}, R_{23}, R_{33}; R_{12}, R_{13}, R_{32}$
$\hat{x}_2$	E_1, E_3	$0^\circ \leqslant \lvert\theta_{13}\rvert < 22.5^\circ$	$R_{11}, R_{31}, R_{13}, R_{33}, \bar{R}_{55}; R_{22}, R_{23}, R_{32}, \bar{R}_{44}$
$\hat{x}_3$	E_3	θ_{12} is indeterminate	R_{13}, HOC; R_{23}
		Noncentrosymmetric-uniaxial-hexagonal $\bar{6}m2(m\perp\hat{x}_2)$	
$\hat{x}_1$	E_2, E_3	$0^\circ \leqslant \lvert\theta_{23}\rvert < 22.5^\circ$	$R_{22}, R_{32}, R_{23}, R_{33}, \bar{R}_{44}; R_{11}, R_{31}, R_{13}, \bar{R}_{55}$
$\hat{x}_2$	E_2, E_3	$\theta_{13} = 0^\circ$	$R_{12}, R_{32}, R_{13}, R_{33}; R_{21}, R_{31}, R_{23}$
$\hat{x}_3$	E_3	θ_{12} is indeterminate	R_{13}, HOC; R_{23}
		Noncentrosymmetric-uniaxial-hexagonal $6mm$	
$\hat{x}_1$	E_1	$\theta_{23} = 0^\circ$	$R_{21}, R_{31}; R_{12}, R_{32}$
$\hat{x}_2$	E_2	$\theta_{13} = 0^\circ$	$R_{12}, R_{32}; R_{21}, R_{31}$
$\hat{x}_3$	E_1, E_2	$\theta_{12} = \frac{1}{2}\arctan(\frac{E_1E_2}{E_1^2-E_2^2})$	$R_{11}, R_{12}; R_{66}, R_{22}, R_{21}$
		Noncentrosymmetric-anaxial-cubic 23 and $\bar{4}3m$	
$\hat{x}_1$	E_2, E_3	$0^\circ \leqslant \lvert\theta_{23}\rvert \leqslant 45^\circ$	$R_{22}, R_{23}, R_{32}, R_{33}, R_{44}; R_{11}, R_{12}, R_{13}, R_{21}, R_{31}, R_{55}, R_{66}$
$\hat{x}_2$	E_1, E_3	$0^\circ \leqslant \lvert\theta_{13}\rvert \leqslant 45^\circ$	$R_{11}, R_{13}, R_{31}, R_{33}, R_{55}; R_{22}, R_{23}, R_{32}, R_{21}, R_{12}, R_{44}, R_{66}$
$\hat{x}_3$	E_1, E_2	$0^\circ \leqslant \lvert\theta_{12}\rvert \leqslant 45^\circ$	$R_{11}, R_{12}, R_{21}, R_{22}, R_{66}; R_{33}, R_{23}, R_{32}, R_{31}, R_{13}, R_{44}, R_{55}$

in each of the 18 remaining point groups not having inversion symmetry properties.

The "Electro-optic coefficients" column contains only Kerr coefficients; these generic moduli could correspond to either clamped (high-fequency, strain-free) or unclamped (low-frequency, stress-free) quadratic coefficients, depending on the actual experimental setup. The moduli with a bar on top ($\bar{R}$) belong to squared Kerr terms which, in the nonzero-natural-birefringence approximations [Eqs. (6) and (7)], introduce net quartic electro-optic contributions (10^{-24}–10^{-6}) to the values of the new (eigen)indexes of refraction. Each row of Table I corresponds to a different setup configuration. The

electric field components that do not show up in a particular table cell are considered null by default; the components that are mentioned are not to be considered zero all at the same time. The Kerr coefficients at each row's end are divided into two sets by a semicolon. The first set contains all the different quadratic electro-optic coefficients which are explicitly involved through nonlinear combinations in the expressions for the new (eigen)indexes of refraction to be determined for that specific configuration; the second set contains second-order electro-optic moduli which are related to the coefficients in the first set through symmetry properties specific to that particular point group. In most of the cases, the inclination angle θ_{pq} is dependent on both the Kerr coefficients and the strength of the electric field's components; its magnitude usually varies between 0° and 45°. In some situations, however, the angle depends only on the Kerr coefficients, while in others, it depends only on the electric field's components. The configurations for which the inclination angle is indeterminate correspond to the physical cases in which the index ellipse is actually an index circle; in these kinds of situations, the values of the refractive index (the radius of the index circle) still depend only on the Kerr effect. Since the electrically induced (optical) phase difference between the fast and slow polarizations in these particular types of setups remains zero up to the third-order (cubic) electro-optic dependence, these cases could in principle allow for the possibility of going beyond the quadratic effect and obtaining some direct information about the higher-order coefficients (HOC) using polarimetric [1–9,11–21] and/or ellipsometric methods [11]; the Kerr effect, which still happens to be isotropically present in the plane of the index circle, could be detected using interferometric techniques [11–13]. In Sec. II, in the nonzero-natural-birefringence cases [Eqs. (6) and (7)], the terms $|n'^{-2}_{pp} - n'^{-2}_{qq}| \cong |n^{-2}_{pp} - n^{-2}_{qq}|$ are considered to be much greater than any electro-optic effect contributions ($>10^{-3} \gg 10^{-12}$); the same is not true for the zero-natural-birefringence situations [Eqs. (4), (5), (11), and (12)] treated in Secs. II and III.

On the practical side, and to the best of the authors' knowledge, the first determinations of some individual Kerr coefficients for (uniaxial) tetragonal (4*mm*) barium titanate ($BaTiO_3$) have been done outside the traditional electro-optics field using a powerful nonlinear optics technique involving degenerate four-wave mixing (DFWM) [43]; surprisingly enough, this method ends up making use of Pockels coefficient values when calculating the (cascaded) contributions to the third-order (effective) nonlinear susceptibilities (Kerr moduli). In the present work, however, the authors have theoretically shown that just by using conventional electro-optics detection procedures [2–21], it is possible in principle to do without the involvement of any Pockels coefficients when trying to detect certain Kerr contributions in 90% of the point group crystal classes which lack a center of symmetry. In this regard, the authors experimentally obtained some individual numerical values for two Kerr coefficients of ferroelectric barium titanate (tetragonal 4*mm*) using a polarimetric (electro-optic) technique [44,45] The values measured, $R_{31} = -8.0 \pm 0.7 \times 10^{-17}$ m^2 V^{-2} and $R_{21} = -3.5 \pm 0.3 \times 10^{-17}$ m^2 V^{-2}, fall within the wide range of quadratic electro-optic coefficients (10^{-24} m^2 V^{-2} to 10^{-15} m^2 V^{-2}) mentioned in the contemporary crystal physics literature [2–9,11–13,22] mostly for centrosymmetric materials. Relative to some of the Kerr moduli obtained by Biaggio [43], however, the authors' values are about 3 orders of magnitude greater. The discrepancy between the two groups' measured coefficients could be due to at least one of the three main factors: high dispersion—in the case of DFWM—because of very high modulation frequency corresponding to the beam's electric field [6], crystal damage, twinning, and/or asymmetric polling induced by a high (DC) field amplitude [44,45], and growth- or fabrication-induced misalignment of the initial indicatrix relative to the cut faces of the crystal [46,47]. The first factor is negligible in traditional low-power–low-frequency electro-optics [2–20]. In the authors' experience, for barium titanate, the second factor could be kept under control for amplitudes of the applied (DC) electric field less than 6×10^5 Vm^{-1}. Sometimes crystal damage, twinning, and nonuniform polling can be prompted by the accumulation of residual charge on the faces of the crystal; this surface charge problem can be solved by applying a low-frequency alternative voltage across the material sample on top of a zero-frequency (DC) field [11–13]; the AC voltage device can be synchronized with the measuring aparatus through the means of a lock-in amplifier. The third and least controllable of all the preceding factors can have its influence minimized by the growing or procuring of very high quality, millimeter-thick crystals having all faces finely cut and smoothly polished such as the photorefractive-grade type in the particular case of ferroelectric (tetragonal 4 mm) $BaTiO_3$ [48,49].

VI. CONCLUSION AND OUTLOOK

The theoretical tabulated findings of this article constitute a contribution to the century-old field of electro-optics (Kerr 1875, Pockels 1893) which, until presently [1–35], has unfortunately failed to take into extensive consideration the (sometimes subtle) possibilities of obtaining direct information about (pure) quadratic effects without any (conspicuous or inconspicuous) contributions involving linear coefficients in most of the point group classes lacking inversion symmetry. The major theoretical application of this work is the extension of the general idea and treatment used here in the case of the electro-optic effect to other phenomena of crystal physics in which a higher order (phenomenological) effect is usually eclipsed by a lower-order one; these other physical phenomena to be studied and analyzed could be optical, electrical, magnetic, mechanical, thermal or chemical-stoichiometric in nature [1–13,18,20,22–35].

The main practical application will be the demanding task of systematic measurement and numerical tabulation of the sets of Kerr coefficients presented in Table I; the real-time monitoring of these (sets of) moduli under changing external factors, such as temperature, could provide researchers with extra information regarding the dynamics of phase transitions. In addition, many of the HOC configurations in Table I constitute good experimental opportunities for determination of other (secondary) optical effects associated with the application of electric fields across (noncentrosymmetric) crystals such as the electrically induced dichroism and the electrogyration effect [2,4,11,25,50].

The challenging—but not impossible—project involving the direct determination and tabulation of Kerr moduli and, by extension, of other (sets of) optical or non-optical (genuinely) quadratic coefficients in noncentrosymmetric materials has a good chance of becoming quite involved in the future because of the vast number of crystals and minerals which fall within the point group symmetry classes treated in Table I. The project's theoretical and practical implications could lead, directly or indirectly, to an improvement in the general body of knowledge and applications with regard to the multitude of (phenomenological) macroscopic optical and nonoptical physical properties of materials in all the condensed matter subfields which deal with organic or inorganic, soft or solid substances lacking inversion symmetry.

[1] J. F. Nye, *Physical Properties of Crystals: Their Representation by Tensors and Matrices* (Oxford University Press, Oxford, 1985).

[2] A. Yariv and P. Yeh, *Optical Waves in Crystals: Propagation and Control of Laser Radiation* (Wiley, Hoboken, 2003).

[3] A. Yariv and P. Yeh, *Photonics: Optical Electronics in Modern Communications* (Oxford University Press, New York, 2007).

[4] S. Huard, *Polarization of Light* (Wiley, Chichester, 1997).

[5] D. R. Lovett, *Tensor Properties of Crystals* (IOP, Bristol, 1999).

[6] B. E. A. Saleh and M. C. Teich, *Fundamentals of Photonics* (Wiley, Hoboken, 2007).

[7] D. Goldstein, *Polarized Light* (Marcel Dekker, New York, 2003).

[8] R. L. Sutherland, *Handbook of Nonlinear Optics* (Marcel Dekker, New York, 2003).

[9] R. E. Newnham, *Properties of Materials: Anisotropy, Symmetry, Structure* (Oxford University Press, New York, 2005).

[10] R. F. Tinder, *Tensor Properties of Solids: Phenomenological Development of the Tensor Properties of Crystals* (Morgan & Claypool Publishers, San Francisco, 2008).

[11] F. Agullo-Lopez, J. M. Cabrera, and F. Agullo-Rueda, *Electrooptics: Phenomena, Materials, and Applications* (Academic, San Diego, 1994).

[12] S. Haussühl, *Physical Properties of Crystals: An Introduction* (Wiley-VCH, Weinheim, 2007).

[13] H.-J. Weber, in *Crystals: Growth, Properties, and Applications*, edited by H. C. Freyhardt (Springer, Berlin, 1988).

[14] C. C. Davis, *Lasers and Electro-optics: Fundamentals and Engineering* (Cambridge University Press, Cambridge, 1996).

[15] K. Iizuka, *Elements of Photonics: In Free Space and Special Media* (Wiley, New York, 2002), Vol. 1.

[16] Y. B. Band, *Light and Matter: Electromagnetism, Optics, Spectroscopy, and Lasers* (Wiley, Chichester, 2007).

[17] R. Guenther, *Modern Optics* (Wiley, New York, 1990).

[18] T. S. Narasimhamurty, *Photoelastic and Electro-optic Properties of Crystals* (Plenum, New York, 1981).

[19] I. P. Kaminow, *An Introduction to Electrooptic Devices* (Academic, Orlando, 1974).

[20] D. F. Nelson, *Electric, Optic, and Acoustic Interactions in Dielectrics* (Wiley, New York, 1979).

[21] H. A. Haus, *Waves and Fields in Optoelectronics* (Prentice Hall, Inc., Upper Saddle River, New Jersey, USA, 1983).

[22] H. J. Juretschke, *Crystal Physics: Macroscopic Physics of Anisotropic Solids* (Benjamin, Reading, 1974).

[23] W. P. Mason, *Crystal Physics of Interaction Processes* (Academic, New York, 1966).

[24] V. M. Agranovich and V. L. Ginzburg, *Crystal Optics with Spatial Dispersion and Excitons* (Springer, Berlin, 1984).

[25] B. N. Grechushnikov, in *Modern Crystallography IV: Physical Properties of Crystals*, edited by L. A. Shuvalov (Springer, Berlin, 1988).

[26] A. M. Glazer and K. G. Cox, in *International Tables for Crystallography: Physical Properties of Crystals*, edited by A. Authier (Kluwer Academic, Dordrecht, 2003).

[27] D. Schwarzenbach, *Crystallography* (Wiley, Chichester, 1996).

[28] M. Catti, in *Fundamentals of Crystallography*, edited by C. Giacovazzo (Oxford University Press, Oxford, 2002).

[29] L. D. Landau, E. M. Lifshitz, and L. P. Pitaevskii, *Electrodynamics of Continuous Media* (Elsevier Butterworth-Heinemann, Oxford, 2008).

[30] A. S. Nowick, *Crystal Properties via Group Theory* (Cambridge University Press, Cambridge, 1995).

[31] W. A. Wooster, *Tensors and Group Theory for the Physical Properties of Crystals* (Oxford University Press, London, 1973).

[32] S. Bhagavantam, *Crystal Symmetry and Physical Properties* (Academic, London, 1966).

[33] A. R. Billings, *Tensor Properties of Materials: Generalized Compliance and Conductivity* (Wiley Interscience, London, 1969).

[34] S. V. Popov, Y. P. Svirko, and N. I. Zheludev, *Susceptibility Tensors for Nonlinear Optics* (IOP, Bristol, 1995).

[35] Y. P. Svirko and N. I. Zheludev, *Polarization of Light in Nonlinear Optics* (Wiley, Chichester, 1999).

[36] S. Ducharme, J. Feinberg, and R. R. Neurgaonkar, IEEE J. Quantum Electron. **23**, 2116 (1987).

[37] M. Melnichuk and L. T. Wood, J. Opt. Soc. Am. A **23**, 1236 (2006).

[38] M. Izdebski and W. Kucharczyk, J. Opt. Soc. Am. B **25**, 149 (2008).

[39] [http://www.newport.com].

[40] [http://www.thorlabs.com].

[41] E. E. Wahlstrom, *Optical Crystallography* (Wiley, New York, 1969).

[42] W. D. Nesse, *Introduction to Optical Mineralogy* (Oxford University Press, New York, 2004).

[43] I. Biaggio, Phys. Rev. Lett. **82**, 193 (1999).

[44] M. Melnichuk and L. T. Wood, J. Opt. Soc. Am. A **22**, 377 (2005).

[45] M. Melnichuk and L. T. Wood, J. Opt. Soc. Am. A **24**, 2843 (2007).

[46] M. Izdebski and W. Kucharczyk, Opto-Electron. Rev. **16**, 42 (2008).

[47] M. Izdebski, Appl. Opt. **47**, 2729 (2008).

[48] [http://www.mtixtl.com].

[49] [http://marketech-crystals.com].

[50] O. G. Vlokh and R. O. Vlokh, Opt. Photonics News **20**(4), 34 (2009).